Review

Microbubble Delivery Platform for Ultrasound-Mediated Therapy in Brain Cancers

Kibeom Kim [1] , **Jungmin Lee** [2] **and Myoung-Hwan Park** [1,2,3,4,*]

1   Department of Chemistry and Life Science, Sahmyook University, Seoul 01795, Republic of Korea
2   Convergence Research Center, Nanobiomaterials Institute, Sahmyook University,
    Seoul 01795, Republic of Korea
3   Department of Convergence Science, Sahmyook University, Seoul 01795, Republic of Korea
4   N to B Co., Ltd., Seoul 01795, Republic of Korea
*   Correspondence: mpark@syu.ac.kr

Abstract: The blood-brain barrier (BBB) is one of the most selective endothelial barriers that protect the brain and maintains homeostasis in neural microenvironments. This barrier restricts the passage of molecules into the brain, except for gaseous or extremely small hydrophobic molecules. Thus, the BBB hinders the delivery of drugs with large molecular weights for the treatment of brain cancers. Various methods have been used to deliver drugs to the brain by circumventing the BBB; however, they have limitations such as drug diversity and low delivery efficiency. To overcome this challenge, microbubbles (MBs)-based drug delivery systems have garnered a lot of interest in recent years. MBs are widely used as contrast agents and are recently being researched as a vehicle for delivering drugs, proteins, and gene complexes. The MBs are 1–10 μm in size and consist of a gas core and an organic shell, which cause physical changes, such as bubble expansion, contraction, vibration, and collapse, in response to ultrasound. The physical changes in the MBs and the resulting energy lead to biological changes in the BBB and cause the drug to penetrate it, thus enhancing the therapeutic effect. Particularly, this review describes a state-of-the-art strategy for fabricating MB-based delivery platforms and their use with ultrasound in brain cancer therapy.

Keywords: microbubble; ultrasound; brain cancer; blood-brain barrier; drug delivery

1. Introduction

The blood-brain barrier (BBB) is a unique interface composed of blood capillaries in the central nervous system (CNS) that maintains homeostasis in the neural microenvironment and protects the brain parenchyma from foreign toxic substances [1–7]. Tight junctions between the brain capillaries and endothelial cells (ECs) prevent the transport of molecules, except for small-sized molecules and lipid molecules, into the brain. In addition to the tight junctions, the brain capillary ECs, which have extraordinarily low transcytosis rates and no fenestrations, inhibit the transcellular transport of macromolecules [8–15]. In the treatment of brain cancers, chemotherapy is a major treatment method for suppressing cancer expression to prevent cancer recurrence after surgical resection [16,17]. However, the barrier properties of the BBB and efflux transporters P-glycoproteins and breast cancer-resistant proteins that are highly expressed in BBB are the primary cause hindering the delivery of drugs to the CNS for cancer treatment [12,18]. Therefore, although several studies have been conducted on approaches for delivering anticancer drugs to the CNS, limitations such as high invasiveness, poor distribution, insufficient efficacy, and intolerable toxicity remain [12].

Due to the unique structure of the brain, the treatment of brain-related diseases has involved various technological attempts to overcome this hindrance effectively by promoting drug delivery to the CNS [2,19]. Among these attempts, thermal ablation using high temperature generated by focused ultrasound energy, whose safety and efficacy have

been verified, is being actively attempted worldwide as a surgical treatment for brain diseases such as obsessive-compulsive disorder, mental disorders such as depression, and intractable pain [20–23]. Particularly, various clinical trials have been conducted to treat brain diseases effectively by promoting drug delivery to the CNS via control of the BBB through the stable and inertial cavitation phenomenon of microbubbles (MBs) that occur when focused ultrasound is applied to the cerebral blood vessels [24–26]. Additionally, the MB-based system is of great interest for the effective delivery of drugs across the BBB due to its non-invasive, transient, reversible, and localized properties [27–32].

In the 1930s, Dr. Karl Dussik first published a paper on the use of ultrasound to visualize cerebral ventricles in the brain by measuring reflections of ultrasound through the head and in the late 1960s, Dr. Claude Joyner first noted the development of MBs as a contrast medium, and the clinical use of MBs started after Gramiak and Shah acknowledged this subject [33–35]. However, the vast potential of MBs as drug-delivery vehicles was recognized only in the late 1990s [36–38]. The structure of the MBs comprises an inner center (core) and an outer layer (shell). MBs physically interact with the surrounding medium through stable cavitation or inertial cavitation, depending on the ultrasound intensity used. On the one hand, stable cavitation generated by ultrasound excitation causes continuous oscillation, which induces a liquid flow around the MBs. On the other hand, inertial cavitation at higher ultrasonic intensities results in the implosion or collapse of the MBs, generating violent mechanical stresses, microjets, and shock waves [17,39–43]. In addition, since the required acoustic energy and response differ depending on the size and concentration of microbubbles, the physical parameters of ultrasound, such as period per pulse, pulse amplitude, pulse repetition frequency, and exposure length, must be adjusted to determine the optimal ultrasound and microbubble combination [44,45]. These phenomena induce biological changes in the BBB, such as increased endocytosis/transcytosis, paracellular passage, and opening of the tight junctions, thus increasing the permeability of the BBB macrostructure for brain cancer therapy [17,46–49]. This review investigated the generation methods, constituent materials, and various studies on MBs for brain cancer treatment (Scheme 1).
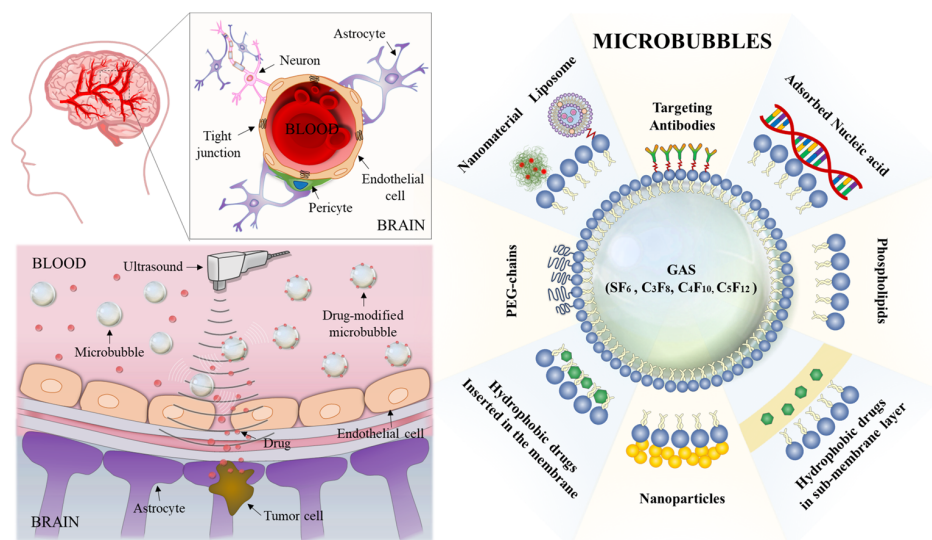
Scheme 1. Illustration of the structure of the microbubbles and the drug delivery mechanism through the blood-brain barrier by the opening effect of the microbubbles.

2. Structure and Composition of MBs

The structure of the MBs comprises the core and shell structures, each with different physicochemical properties. Various materials have been used as the core and shell structural components to increase the stability and efficiency of MBs for brain cancer therapy [34,50].

2.1. Core Structure

The first-generation MBs had low stability in solution because atmospheric air constituted the core, and they lacked a stabilizing shell. The stability was increased in the next generation of MBs by incorporating a shell; however, MBs that have an air core have low stability in the biological environment because air dissolves in the blood [38,51,52]. Therefore, in brain cancer therapy, sulfur hexafluoride (SF$_6$) or perfluorocarbons, which have higher molecular weights and lower blood solubility than those of atmospheric air, are used as the core in MBs. SonoVue® (SF$_6$), Definity® (perfluoropropane [C$_3$F$_8$]), and Optison® (C$_3$F$_8$), which are commercially used, have a perfluorochemical as the material constituting the core. Additionally, other studies have utilized perfluorochemicals such as perfluorobutane (C$_4$F$_{10}$) and perfluoropentane (C$_5$F$_{12}$) as the core components [38,52]. Particularly, C$_5$F$_{12}$, a volatile gas with a boiling point of 26 °C, exists in liquid form during the MBs' manufacturing process and forms the MBs while changing to the gaseous state at body temperature after injection [34,38,52,53].

2.2. Shell Structure

The shell structure comprises polymers, proteins, surfactants, or phospholipids to prevent gas leakage, breakdown, and coalescence [34,36,53,54]. Notably, the shell structure significantly reduces the surface tension of MBs, which is closely related to their stability [54–56]. The water and gas molecules at the MB gas–water interface form hydrogen bonds horizontally along the interface line. This creates a contraction force on the surface of the MBs, which generates surface tension in the inward direction and induces an increase in the pressure inside them. Higher pressure increases the dissolution rate of the gas, reducing the stability of the MBs. The shell structure that covers the surface of the core increases the stability of the MBs by preventing the formation of ordered hydrogen bonds and reducing the inner pressure of the MBs [28,38,53,56].

The constituent shell materials mainly used in the brain cancer therapy system are phospholipids and phospholipid derivatives. Moreover, a broad range of phospholipids with various hydrophobic chain lengths and electrostatic charges have been utilized [53,57,58]. Thus, it facilitates the customization of the system according to the characteristics of the delivered material. The hydrophobicity of phospholipids affects the drug-loading capacity and stability of the MBs [59]. Moreover, polyethylene glycol-modified phospholipid (PEG-PL) endows the MBs with a stealth effect to evade clearance by the reticuloendothelial system Phospholipids such as dipalmitoyl phosphoric acid (DPPA), dipalmitoylphosphatidylethanolamine (DPPE), dipalmitoylphosphatidylcholine (DPPC), dipalmitoylphosphatidylglycerol (DPPG), distearoylphosphatidylcholine (DSPC), and distearoylphosphatidylglycerol (DSPG) are used to form the shell of the MBs (Figure 1).
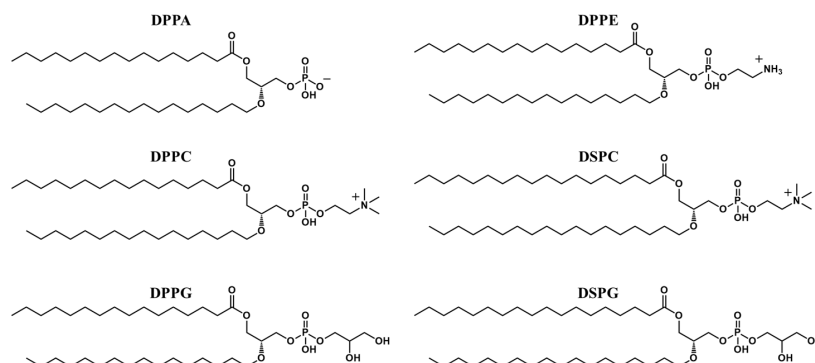

Figure 1. Structure of phospholipids used in microbubble synthesis. (DPPA, dipalmitoyl phosphoric acid; DPPE, dipalmitoylphosphatidylethanolamine; DPPC, dipalmitoylphosphatidylcholine; DPPG, dipalmitoylphosphatidylglycerol; DSPC, distearoylphosphatidylcholine; DSPG, distearoylphosphatidylglycerol).

2.3. Multi-Functionalization of MBs

The effects of brain cancer therapy can be enhanced by modifying the MBs comprising a core and shell with cancer drugs, cancer-targeting ligands, DNA, and nanomedicine. These materials develop an association with the MBs shell via electrostatic or hydrophobic interactions, van der Waals forces, physical encapsulation, host-guest interactions, or covalent bonds [28,38,60,61]. Furthermore, functionalized MBs' structures were designed by modifying the material properties and interactions between the MBs. Hydrophilic DNA is attached to the surface of the MBs comprising positively charged lipid shells via electrostatic interactions (Scheme 2a) [62]. Lipophilic or hydrophobic drugs can be encapsulated in the phospholipid shells (Scheme 2b) [63–65]. The host-guest interaction of avidin-biotin was used to modify the targeting ligand on the MBs' surface (Scheme 2c) [62,65]. Because the surface area or shell volume of the MBs is restricted, modification of the liposomes on the MBs' surface provides a larger space for accommodating medicinal materials (Scheme 2d) [28,66–70].
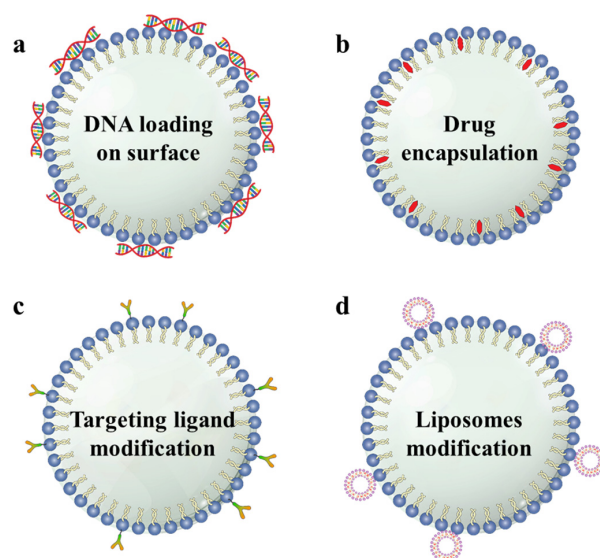
Scheme 2. Illustration of the various structures of functionalized microbubbles. (**a**) DNA can be loaded on the surface of the MBs (**b**) Hydrophobic drugs can be encapsulated in the shell of the MBs. (**c**) Targeting ligands can be modified to the surface of the MBs. (**d**) Drug-loaded liposomes can be attached to the surface of the MBs. (MB, microbubble).
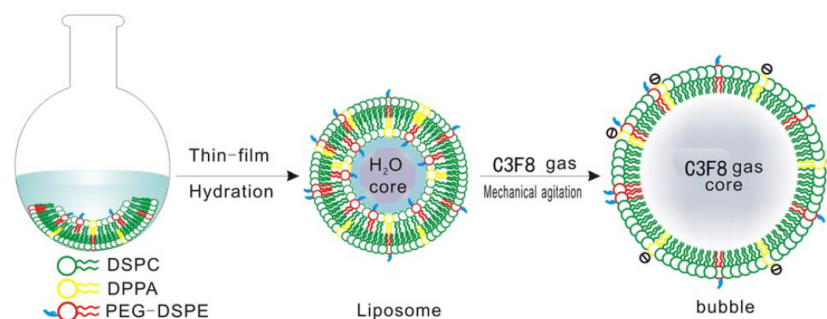
3. Fabrication Method

3.1. Sonication Method

This method uses high-intensity ultrasound to generate MBs after dispersing the gas constituting the core in a liquid containing an appropriate coating material that forms the shell for stabilizing the MBs. The size distribution of the generated MBs depends on the frequency, power, and pulse region of the ultrasound; however, the theoretical relationship between these parameters and fabrication protocols has not been elucidated and has been developed empirically. The material is used as the outer shell and dissolved in the aqueous solution, and sonication is applied. Gas is continuously supplied to the solution for MBs generation. After generating the MBs using sonication, centrifugation and/or filtration are required to remove the residual substances [34,71–73].

3.2. Thin-Film Hydration Method

A solution of the material used as the outer shell and dissolved in a volatile solvent is evaporated to remove the solvent, and a thin film is formed on the surface of the container. After preparing a liposome solution by adding a water-soluble solvent to the container on which the thin film is formed, it is transferred to a hermetic vial filled with

the gas constituting the core and then mechanically mixed to produce MBs. After the generation of MBs, the residues dispersed in the solution are removed via centrifugation (Scheme 3) [70,74,75].

Scheme 3. Illustration of the process of the thin film-hydration method. (DPPA, dipalmitoyl phosphoric acid; DSPC, distearoylphosphatidylcholine; PEG–DSPE, polyethylene glycol–1, 2-distearoyl-sn-glycero-3-phosphoethanolamine). Reproduced with permission from [75] (Copyright © 2018, John Wiley & Sons, Inc.).

3.3. Membrane Emulsification Method

MBs are formed at the pore outlet under a high-pressure state and are detached from the membrane by the shearing force applied by the solution containing the shell constituent material flowing in the continuous phase (Scheme 4). The advantage of this method is that it produces MBs with a narrower size distribution than that of the aforementioned sonication and thin-film hydration methods. The size and size distribution depend on the membrane pore size, surface properties of the membrane, shear stress, transmembrane pressure, and substrate composing solution in the continuous phase [76,77].
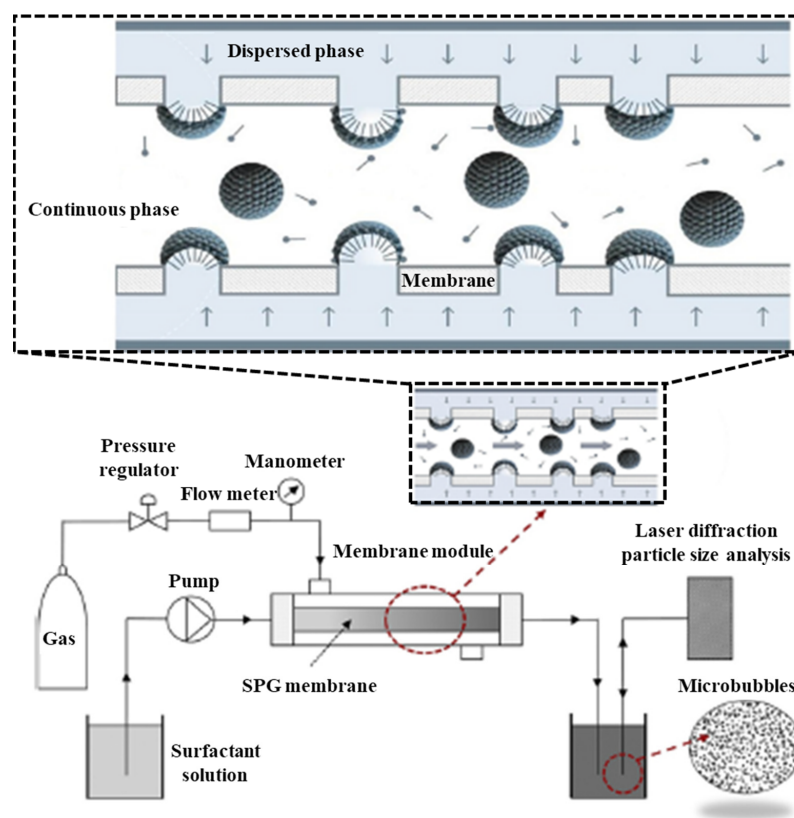
Scheme 4. Illustration of the thin-membrane emulsification method (SPG, Shirasu porous glass) Reproduced with permission from [77] (Copyright © 2019, Elsevier B.V.).

3.4. Microfluidics Method

Although microfluidics has the advantage of generating narrow size distribution of MBs, it has restricted generation parameters and low productivity. The gas stream and the stream of the solution containing the shell component meet at the orifice, which is a feature of microfluidic devices. The MBs are then formed at a certain distance by a "pinch off" phenomenon (Figure 2). The generation of MBs is controlled by several parameters, such as the flow rate, viscosity ratios of gas and continuous phases, and the number of capillaries [78–81].
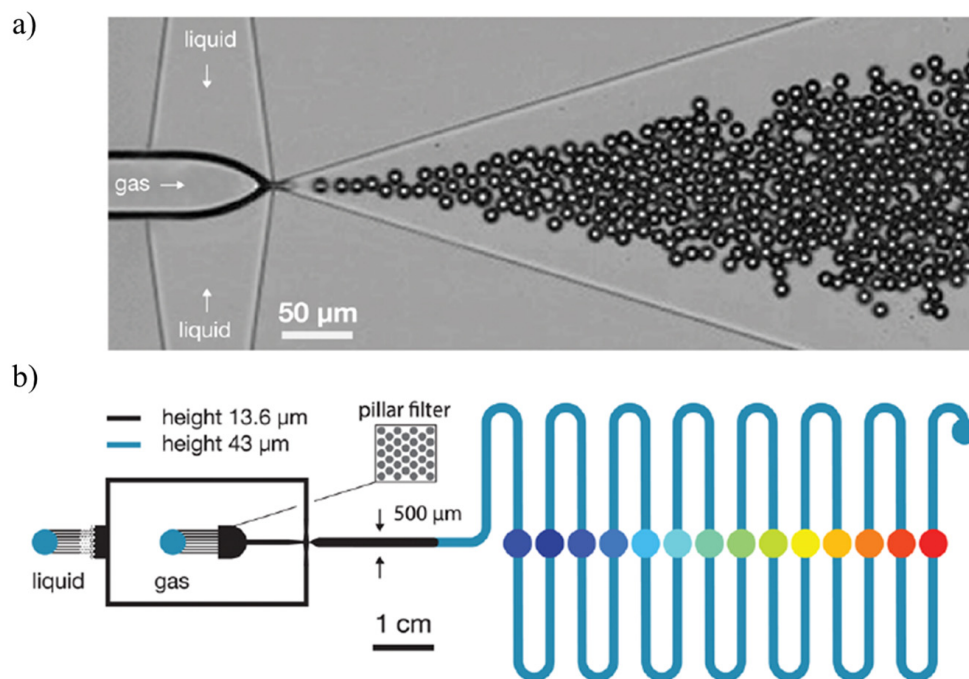

Figure 2. Bubble formation at a rate of 6×10^4 bubbles/s from a flow focusing (**a**) connected to a serpentine channel 15 cm in length (**b**) to characterize the bubble stability over the first minute after their formation. Reproduced with permission from [78] (Copyright © 2016, American Chemical Society).

4. Utilizing Methods of MBs

MBs can be co-injected with various drugs or drug delivery platforms to increase the BBB permeability toward the drugs under ultrasound irradiation [82–88]. The co-injection method is advantageous, as it can be used together with the existing drug delivery systems and commercially available MBs to perform diverse treatments [89–92]. Moreover, MBs can be used as a drug delivery vehicle by loading a drug on a shell [63,86]. In this method, the MBs collapsed by ultrasound irradiation not only open the BBB but also release the loaded drugs, enabling stimuli-responsive drug release, which can increase the therapeutic effect. In this section, the MB-based platforms used for brain cancer therapy are summarized.

4.1. Co-Injection of MBs with Drugs

Co-injection of MBs and drugs induces a therapeutic effect against brain cancer by increasing BBB penetration. Commercially available MBs contrast agents, such as SonoVue®, Definity®, and Optison®, are used in the co-injection method that facilitates the delivery of cancer drugs, proteins, cells, and metal nanoparticles to the CNS [93–96]. MBs are co-injected with anticancer drugs to improve the therapeutic efficacy and diagnosis [91,92,97–101]. Kuo et al. confirmed the BBB opening effect by ultrasound and MBs on magnetic resonance imaging (MRI) [91]. Changes in the MRI intensity were observed after the co-injection of MRI contrast agents, gadopentetic acid (Gd-DTPA) and SonoVue®. The

BBB opening effect by MBs and ultrasound enhanced the MR signal intensity by increasing the Gd-DTPA permeability. Additionally, the temozolomide (TMZ) concentration ratio in the cerebrospinal fluid (CSF) and plasma was observed to confirm the BBB-opening effect. The concentration ratio of TMZ in the CSF/plasma was 22.7% in the TMZ alone group, while that in the MB/ultrasound group increased to 33.6%. This result indicates that the BBB permeability of the drug increased owing to the BBB opening effect. Furthermore, Daniel et al. researched the effective treatment of brain cancer using SonoVue® and paclitaxel (PTX) [102]. Although PTX is one of the anticancer drugs used in various cancer treatments, it has limited benefits in brain cancer due to its poor BBB permeability. The BBB-opening effect of MBs facilitates the penetration of PTX into the BBB and enhances its efficacy in brain cancer treatment. These results were observed in tumor-bearing mice. Tao et al. conducted an experiment to enhance drug delivery using Optison® [103]. By observing the cavitation behavior of MBs, an experiment was conducted to prevent brain damage and deliver the drug effectively, and this was confirmed in an F98 rat glioma model. Hyungwon et al. studied the co-injection effect of SonoVue® and drug-loaded ultrasound-sensitive liposomes [104]. An ultrasound-sensitive liposome is produced using the thin-film hydration method. Doxorubicin (Dox) is encapsulated in the liposome vesicles, which increase the drug biostability and release drugs in response to ultrasound. The released drug is delivered to the CNS by the BBB-opening effect of the MBs, facilitating chemotherapy for brain cancer.

The co-injection method of MBs is not limited to chemotherapy through the delivery of anticancer drugs but enables various therapies by allowing several substances to penetrate the CNS. Immune checkpoint inhibition (ICI) therapies, which target programmed cell death ligand 1 (PD-L1), programmed cell death-1, and cytotoxic T lymphocyte-associated protein-4, have been approved by the United States Food and Drug Administration for the treatment of various cancers. However, ICI therapies have limited efficacy in brain cancers [105,106]. Although the mechanisms underlying this failure remain unclear, the BBB is considered one of the obstacles in performing ICI therapy for brain cancer. Yan et al. investigated ICI therapy for brain cancer treatment using Definity® and anti-PD-L1 (aPD-L1), which is an immune checkpoint inhibitor [107]. The effect of BBB opening by MBs and ultrasound increased the CNS delivery rate of aPD-L1, thus proving the possibility of applying ICI therapy in brain cancer cases. Moreover, it was confirmed that the injection method of MBs and control of the sonication pattern affect the delivery rate of aPD-L1 and the effects of ICI therapy. However, as the study was conducted on wild-type mice, additional in vivo experiments in brain cancer models are needed to verify this effect. Ryan et al. conducted experiments on BBB penetration of natural killer (NK)-92 cells for brain cancer therapy [108]. These cells are cytotoxic lymphocytes involved in the innate immune response against malignant cells. Decreased tumor size and increased survival rate in the rats were observed in the Definity® and NK-92 cells treatment groups.

The BBB penetration by metal nanoparticles can be increased by the BBB-opening effect [109]. In the study by Dezhuan et al., MBs consisting of phospholipids, C_4F_{10}, and ^{64}Cu-Au clusters were injected into the mice, and the BBB penetration effect was observed through positron emission tomography [110]. Pin et al. used carmustine-modified iron nanoparticles and SonoVue® to facilitate MRI diagnosis and chemotherapy [111]. Carmustine is immobilized on the surface of iron nanoparticles by forming a covalent bond. The co-injection of the prepared nanoparticles and MBs facilitates the MRI monitoring of drug delivery and brain cancer therapy. This experiment was conducted using the B6 rat glioma model. Table 1 summarizes the types of MBs, constituent materials, drugs, cells, and animals used in the research that utilized the co-injection method.

Table 1. Summary of the types of microbubbles, constituent materials, drugs, cells, and animals used in the co-injection method.

MBs	Core	Shell	Drug	Cell/Animal	Reference No.
Definity®	C_3F_8	DPPC, DPPA, PEG-PL	Dox	9L/Rat	[85]
SonoVue®	SF_6	DPPG, DSPC, Palmitic acid	TMZ	9L/Rat	[91]
SonoVue®	SF_6	DPPG, DSPC, Palmitic acid	Dox	GBM8401/Mice	[92]
SonoVue®	SF_6	DPPG, DSPC, Palmitic acid	Interleukin-12	C6/Rat	[95]
SonoVue®	SF_6	DPPG, DSPC, Palmitic acid	Dox	GBM8401/Mice	[97]
SonoVue®	SF_6	DPPG, DSPC, Palmitic acid	TMZ	U87 MG/Mice	[98]
Definity®	C_3F_8	DPPC, DPPA, PEG-PL	Dox	9L/Rat	[99]
Definity®	C_3F_8	DPPC, DPPA, PEG-PL	Dox	9L/Rat	[101]
SonoVue®	SF_6	DPPG, DSPC, Palmitic acid	PTX	GBM12/Mice	[102]
Optison®	C_3F_8	HSA	Dox liposome	F98/Rat	[103]
SonoVue®	SF_6	DPPG, DSPC, Palmitic acid	Dox liposome	U87 MG	[104]
Definity®	C_3F_8	DPPC, DPPA, PEG-PL	anti-PD-L1 antibody	Mice (normal)	[107]
Definity®	C_3F_8	DPPC, DPPA, PEG-PL	NK-92 cell	MDA-MB-231/Rat	[108]
Self-made	C_4F_{10}	DSPC, PEG-PL	^{64}Cu-Au cluster	Mice (Normal)	[110]
SonoVue®	SF_6	DPPG, DSPC, Palmitic acid	Carmustine/Iron nanoparticle	C6/Rat	[111]

(MBs, microbubbles; DPPC, dipalmitoylphosphatidylcholine; DPPA, dipalmitoyl phosphoric acid; PEG-PL, polyethylene glycol-modified phospholipid; Dox, doxorubicin; DPPG, dipalmitoylphosphatidylglycerol; DSPC, distearoylphosphatidylcholine; TMZ, temozolomide; PTX, paclitaxel; HSA, human serum albumin; PD-L1, programmed cell death ligand 1; NK, natural killer).

4.2. MBs as Drug Delivery Vehicles

As mentioned in the aforementioned research, MBs can be used as a material for BBB opening as well as a drug delivery vehicle by conjugating various types of drugs with the MBs. The advantage of conjugating drugs with MBs is the prevention of the degradation of drugs that are unstable in the biological environment and increasing the clinical benefit even at reduced dosages. Furthermore, conjugated drug release is controlled by ultrasound-induced MBs destruction and facilitates targeted drug delivery [63,86]. Chien et al. produced drug-loaded MBs by encapsulating carmustine in the hydrophobic area of the MBs' shells [64]. Carmustine was added during the preparation of the MBs consisting of C_3F_8, DPPC, and PEG-PL. The size of the prepared MBs was 1.11 μm, and their concentration was $19.78 \pm 4.9 \times 10^9$ MBs/mL. It was confirmed that a maximum of 1.67 mg of carmustine was loaded, and the drug encapsulation efficiency was $68.01 \pm 4.35\%$. The MBs system increases the circulating half-life by increasing the biological stability of carmustine, which is easily hydrolyzed in the plasma, and by increasing the delivery rate into the

CNS. Shih et al. observed that drug encapsulation and delivery efficiency depend on the hydrophobicity of the MBs' shell, which was controlled by the length of the phospholipid alkyl chain [112]. The MBs were prepared using C_4F_{10}, DPPC, DSPC, and PEG-PL, and dextran was encapsulated in the MBs' shell. In the delivery of low-molecular-weight (3 kDa) dextran, the hydrophobicity of the shell did not significantly affect the delivery; however, in the delivery of high-molecular-weight (40 kDa) dextran, the higher hydrophobicity of the shell, more effective is the dextran delivery. See et al. generated MBs using SF_6 and a phospholipid with a thiol moiety and then conjugated it with a thiolated liposome containing Dox through a disulfide bond [70]. Following this, a peptide ligand targeting the interleukin 4 receptor, which is overexpressed in brain cancer, was post-modified on the MBs surface to improve the brain cancer-targeting effect. This system effectively targeted and treated U87 MG cancer cells. Boron neutron capture therapy (BNCT) has been receiving increasing attention for treating cancer. BNCT utilizes boronated agents (^{10}B) to treat tumors, which, after undergoing irradiation with neutrons, yields ^7Li and an alpha particle. Since the alpha particle has a short range, it causes irreversible damage to the DNA of the cancer cells without affecting the normal cells [113,114]. To accumulate a sufficient concentration of ^{10}B for brain cancer treatment, it must be manufactured in the form of nanoparticles to utilize the enhanced permeability and retention effect. However, the BBB interrupts nanoparticle delivery to the CNS; thus, the effective delivery of ^{10}B in brain cancer remains an important challenge in BNCT. Ching et al. modified the boron-containing polyanion (polyethylene glycol-b-poly((*closo*-dodecaboranyl)thiomethylstyrene) [PEG-b-PMBSH]) nanoparticles with MBs, which consists of C_3F_8, DPPC, and 1,2-dipalmitoyl-3-trimethylammonium-propane (DPTAP), via electrostatic interaction for BNCT [58]. This MBs-based platform can effectively deliver the PEG-b-PMBSH nanoparticles to the CNS under ultrasound irradiation.

In addition to hydrophobic cancer drugs, metal nanoparticles are encapsulated in the MBs to utilize the unique properties of the nanoparticles for brain cancer therapy. Ching et al. researched a system that facilitates chemotherapy and MRI diagnosis by modifying Dox and superparamagnetic iron oxide (SPIO) in MBs composed of DSPC, DSPG, PEG-PL, and C_3F_8 [63,115]. SPIO and Dox are conjugated by the reaction between the amine group functionalized on the SPIO surface and the carbonyl group of Dox, which are then encapsulated in the MBs' shells [115]. In another study, Dox and SPIO were encapsulated in the MBs' shells without further modification [63]. The MRI signal intensities and brain cancer therapy effects of the systems prepared using the two methods were confirmed in a C6 rat glioma model.

Biological materials with large structures, such as DNA and RNA, can penetrate the BBB by loading onto the MBs. Chang et al. prepared positively charged MBs using DPTAP to load negatively charged DNA onto the surface of the MBs through electrostatic interactions [116]. Additionally, vascular endothelial growth factor receptor 2 antibodies were modified onto the surface of the MBs through an avidin-biotin interaction to increase the gene therapy effect and enhance the cancer-targeting effect. The low BBB permeability of RNA is the main hurdle for utilizing RNA interference therapy against brain cancer. Guanjian et al. prepared the MBs and liposomes conjugated system using the host-guest interaction of avidin-biotin [67]. Before conjugation, short hairpin RNA, which decreases the transcription of the *BIRC5* gene, was loaded onto the liposomes. The effect of RNA interference therapy in brain cancer was confirmed in a C6 rat glioma model.

The use of MBs as a drug vehicle facilitates ultrasound-responsive drug release and increases BBB permeability through the opening effect of the MBs. Table 2 summarizes the types of MBs, manufacturing methods, constituent materials, and loaded drugs used for drug delivery.

Table 2. Summary of the types of microbubbles, constituent materials, manufacturing methods, drugs, cells, and animals used for drug delivery.

MBs	Core	Shell	Preparation Method	Drug	Cell/Animal	Reference No.
Self-made	C_3F_8	DPPC, DPTAP, PEG-PL	Thin film-hydration	Boron nanoparticle	GL261/Mice	[58]
Self-made	C_3F_8	DPPC, DPTAP, PEG-PL	Thin film-hydration	DNA	C6/Rat	[62]
Self-made	C_3F_8	DSPC, DSPG, PEG-PL	Thin film-hydration	Dox	C6/Rat	[63]
Self-made	C_3F_8	DPPC, PEG-PL	Thin film-hydration	Carmustine	C6/Rat	[64]
Self-made	C_3F_8	DPPC, PEG-PL	Thin film-hydration	Carmustine	C6/Rat	[65]
Self-made	C_3F_8	DPPC, PEG-PL	Thin film-hydration	shRNA	C6/Rat	[67]
Self-made	C_3F_8	DPPG, DPPE, PEG-PL	Thin film-hydration	Gambogic acid	U87 MG/Mice	[69]
Self-made	SF_6	DPPC, DPPE, diacetyl phosphate, PEG-PL	Thin film-hydration	Dox	U87 MG	[70]
Self-made	C_4F_{10}	DPPC, DSPC, PEG-PL	Sonication	Dextran	C57/BL mice (normal)	[112]
Self-made	C_3F_8	DSPC, DSPG, PEG-PL	Thin film-hydration	Dox	C6/Rat	[115]

(DPPC, dipalmitoylphosphatidylcholine; DPTAP, 1,2-dipalmitoyl-3-trimethylammonium-propane; PEG-PL, polyethylene glycol-modified phospholipid; DSPC, distearoylphosphatidylcholine; DSPG, distearoylphosphatidyl-glycerol; Dox, doxorubicin; shRNA, short hairpin RNA; DPPG, dipalmitoylphosphatidylglycerol; DPPE, dipalmitoylphosphatidylethanolamine).

5. Conclusions

In the past decade, significant progress has been made in improving the transport of therapeutics across the BBB through reversible opening via MB–ultrasound. This review describes the structure, composition, and preparation methods of the MBs. Hexafluoride (SF_6) or perfluorocarbons, which have low solubility in an aqueous solution, were used as the MBs core to increase the BBB permeation. Various materials can be used as shells to reduce the high surface tension of MBs, but systems used for BBB permeation generally utilize the phospholipid derivatives and introduce PEG moiety to increase biocompatibility and stability. Methods for preparing MBs include sonication, thin-film hydration, membrane emulsification, and microfluidics methods. In the investigated research, sonication and thin-film hydration method were used to generate the MBs. Specifically, the information on drugs used together with MBs, which have recently been used for brain cancer therapy, has been summarized. MBs can be utilized by co-injection with a drug or by directly loading the drug onto them. Utilization of the MB-based systems and ultrasound facilitates the delivery of various medicines, such as anticancer drugs, proteins, liposomes, gene complexes, metal nanoparticles, and cells, to the tumor area in the CNS. Although this technology is in its initial investigation stage and must overcome many challenges before it can be used clinically, it has the potential to improve the therapeutic effect of various treatments that have not been attempted due to the BBB hindrance in the treatment of brain tumors.

Institutional Review Board Statement: Not applicable.

Informed Consent Statement: Not applicable.

Data Availability Statement: Not applicable.

Conflicts of Interest: The authors declare no conflict of interest.

References

1. Lockman, P.; Mumper, R.; Khan, M.; Allen, D. Nanoparticle technology for drug delivery across the blood-brain barrier. *Drug Dev. Ind. Pharm.* **2002**, *28*, 1–13. [CrossRef] [PubMed]
2. Banks, W.A. From blood-brain barrier to blood-brain interface: New opportunities for CNS drug delivery. *Nat. Rev. Drug Discov.* **2016**, *15*, 275–292. [CrossRef] [PubMed]
3. Parodi, A.; Rudzinska, M.; Deviatkin, A.A.; Soond, S.M.; Baldin, A.V.; Zamyatnin, A.A., Jr. Established and Emerging Strategies for Drug Delivery Across the Blood-Brain Barrier in Brain Cancer. *Pharmaceutics* **2019**, *11*, 245. [CrossRef] [PubMed]
4. Steeg, P.S. The blood-tumour barrier in cancer biology and therapy. *Nat. Rev. Clin. Oncol.* **2021**, *18*, 696–714. [CrossRef]
5. Pandit, R.; Chen, L.; Gotz, J. The blood-brain barrier: Physiology and strategies for drug delivery. *Adv. Drug Deliv. Rev.* **2020**, *165–166*, 1–14. [CrossRef]
6. Abbott, N.J. Blood-brain barrier structure and function and the challenges for CNS drug delivery. *J. Inherit. Metab. Dis.* **2013**, *36*, 437–449. [CrossRef]
7. McCrorie, P.; Vasey, C.E.; Smith, S.J.; Marlow, M.; Alexander, C.; Rahman, R. Biomedical engineering approaches to enhance therapeutic delivery for malignant glioma. *J. Control. Release* **2020**, *328*, 917–931. [CrossRef]
8. Schoen Jr, S.; Kilinc, M.S.; Lee, H.; Guo, Y.; Degertekin, F.L.; Woodworth, G.F.; Arvanitis, C. Towards controlled drug delivery in brain tumors with microbubble-enhanced focused ultrasound. *Adv. Drug Delivery Rev.* **2022**, *180*, 114043. [CrossRef]
9. Alonso, A.; Reinz, E.; Jenne, J.W.; Fatar, M.; Schmidt-Glenewinkel, H.; Hennerici, M.G.; Meairs, S. Reorganization of gap junctions after focused ultrasound blood-brain barrier opening in the rat brain. *J. Cereb. Blood Flow Metab.* **2010**, *30*, 1394–1402. [CrossRef]
10. Mitusova, K.; Peltek, O.O.; Karpov, T.E.; Muslimov, A.R.; Zyuzin, M.V.; Timin, A.S. Overcoming the blood-brain barrier for the therapy of malignant brain tumor: Current status and prospects of drug delivery approaches. *J. Nanobiotechnol.* **2022**, *20*, 412. [CrossRef]
11. Agrahari, V.; Agrahari, V.; Mitra, A.K. Nanocarrier fabrication and macromolecule drug delivery: Challenges and opportunities. *Ther. Deliv.* **2016**, *7*, 257–278. [CrossRef] [PubMed]
12. Wu, S.K.; Tsai, C.L.; Huang, Y.; Hynynen, K. Focused Ultrasound and Microbubbles-Mediated Drug Delivery to Brain Tumor. *Pharmaceutics* **2020**, *13*, 15. [CrossRef] [PubMed]
13. Sheikov, N.; McDannold, N.; Sharma, S.; Hynynen, K. Effect of focused ultrasound applied with an ultrasound contrast agent on the tight junctional integrity of the brain microvascular endothelium. *Ultrasound Med. Biol.* **2008**, *34*, 1093–1104. [CrossRef] [PubMed]
14. Liu, H.L.; Fan, C.H.; Ting, C.Y.; Yeh, C.K. Combining microbubbles and ultrasound for drug delivery to brain tumors: Current progress and overview. *Theranostics* **2014**, *4*, 432–444. [CrossRef] [PubMed]
15. Upton, D.H.; Ung, C.; George, S.M.; Tsoli, M.; Kavallaris, M.; Ziegler, D.S. Challenges and opportunities to penetrate the blood-brain barrier for brain cancer therapy. *Theranostics* **2022**, *12*, 4734–4752. [CrossRef]
16. Bai, M.; Dong, Y.; Huang, H.; Fu, H.; Duan, Y.; Wang, Q.; Du, L. Tumour targeted contrast enhanced ultrasound imaging dual-modal microbubbles for diagnosis and treatment of triple negative breast cancer. *RSC Adv.* **2019**, *9*, 5682–5691. [CrossRef]
17. Song, K.H.; Harvey, B.K.; Borden, M.A. State-of-the-art of microbubble-assisted blood-brain barrier disruption. *Theranostics* **2018**, *8*, 4393–4408. [CrossRef] [PubMed]
18. Dasgupta, A.; Liu, M.; Ojha, T.; Storm, G.; Kiessling, F.; Lammers, T. Ultrasound-mediated drug delivery to the brain: Principles, progress and prospects. *Drug Discov. Today Technol.* **2016**, *20*, 41–48. [CrossRef]
19. Stockwell, J.; Abdi, N.; Lu, X.; Maheshwari, O.; Taghibiglou, C. Novel central nervous system drug delivery systems. *Chem. Biol. Drug Des.* **2014**, *83*, 507–520. [CrossRef]
20. Yi, S.; Han, G.; Shang, Y.; Liu, C.; Cui, D.; Yu, S.; Liao, B.; Ao, X.; Li, G.; Li, L. Microbubble-mediated ultrasound promotes accumulation of bone marrow mesenchymal stem cell to the prostate for treating chronic bacterial prostatitis in rats. *Sci. Rep.* **2016**, *6*, 19745. [CrossRef]

21. Isik, U.; Aydogan Avsar, P.; Aktepe, E.; Doguc, D.K.; Kilic, F.; Buyukbayram, H.I. Serum zonulin and claudin-5 levels in children with obsessive-compulsive disorder. *Nord. J. Psychiatry* **2020**, *74*, 346–351. [CrossRef]

22. Lotfi, S.; Patel, A.S.; Mattock, K.; Egginton, S.; Smith, A.; Modarai, B. Towards a more relevant hind limb model of muscle ischaemia. *Atherosclerosis* **2013**, *227*, 1–8. [CrossRef]

23. Wang, F.; Wei, X.X.; Chang, L.S.; Dong, L.; Wang, Y.L.; Li, N.N. Ultrasound Combined With Microbubbles Loading BDNF Retrovirus to Open BloodBrain Barrier for Treatment of Alzheimer's Disease. *Front. Pharmacol.* **2021**, *12*, 615104. [CrossRef] [PubMed]

24. Chien, C.Y.; Xu, L.; Pacia, C.P.; Yue, Y.; Chen, H. Blood-brain barrier opening in a large animal model using closed-loop microbubble cavitation-based feedback control of focused ultrasound sonication. *Sci. Rep.* **2022**, *12*, 16147. [CrossRef]

25. Burgess, M.T.; Apostolakis, I.; Konofagou, E.E. Power cavitation-guided blood-brain barrier opening with focused ultrasound and microbubbles. *Phys. Med. Biol.* **2018**, *63*, 065009. [CrossRef]

26. Kooiman, K.; Roovers, S.; Langeveld, S.A.G.; Kleven, R.T.; Dewitte, H.; O'Reilly, M.A.; Escoffre, J.M.; Bouakaz, A.; Verweij, M.D.; Hynynen, K.; et al. Ultrasound-Responsive Cavitation Nuclei for Therapy and Drug Delivery. *Ultrasound Med. Biol.* **2020**, *46*, 1296–1325. [CrossRef]

27. Klibanov, A.L. Preparation of targeted microbubbles: Ultrasound contrast agents for molecular imaging. *Med. Biol. Eng. Comput.* **2009**, *47*, 875–882. [CrossRef]

28. Ibsen, S.; Schutt, C.E.; Esener, S. Microbubble-mediated ultrasound therapy: A review of its potential in cancer treatment. *Drug Des. Devel. Ther.* **2013**, *7*, 375–388. [CrossRef] [PubMed]

29. Blomley, M.J.; Cooke, J.C.; Unger, E.C.; Monaghan, M.J.; Cosgrove, D.O.J.B. Microbubble contrast agents: A new era in ultrasound. *BMJ* **2001**, *322*, 1222–1225. [CrossRef] [PubMed]

30. Arvanitis, C.D.; Askoxylakis, V.; Guo, Y.; Datta, M.; Kloepper, J.; Ferraro, G.B.; Bernabeu, M.O.; Fukumura, D.; McDannold, N.; Jain, R.K. Mechanisms of enhanced drug delivery in brain metastases with focused ultrasound-induced blood-tumor barrier disruption. *Proc. Natl. Acad. Sci. USA* **2018**, *115*, E8717–E8726. [CrossRef]

31. Mainprize, T.; Lipsman, N.; Huang, Y.; Meng, Y.; Bethune, A.; Ironside, S.; Heyn, C.; Alkins, R.; Trudeau, M.; Sahgal, A.; et al. Blood-Brain Barrier Opening in Primary Brain Tumors with Non-invasive MR-Guided Focused Ultrasound: A Clinical Safety and Feasibility Study. *Sci. Rep.* **2019**, *9*, 321. [CrossRef]

32. Cai, X.; Yang, F.; Gu, N. Applications of magnetic microbubbles for theranostics. *Theranostics* **2012**, *2*, 103–112. [CrossRef]

33. Dussik, K. On the possibility of using ultrasound waves as a diagnostic aid. *Neurol. Psychiat.* **1942**, *174*, 153–168. [CrossRef]

34. Stride, E.; Edirisinghe, M. Novel microbubble preparation technologies. *Soft Matter.* **2008**, *4*, 2350–2359. [CrossRef]

35. Gramiak, R.; Shah, P.M. Echocardiography of the aortic root. *Investig. Radiol.* **1968**, *3*, 356–366. [CrossRef] [PubMed]

36. De Cock, I.; Zagato, E.; Braeckmans, K.; Luan, Y.; de Jong, N.; De Smedt, S.C.; Lentacker, I. Ultrasound and microbubble mediated drug delivery: Acoustic pressure as determinant for uptake via membrane pores or endocytosis. *J. Control. Release* **2015**, *197*, 20–28. [CrossRef] [PubMed]

37. Teng, W.; Huneiti, Z.; Machowski, W.; Evans, J.; Edirisinghe, M.; Balachandran, W. Towards particle-by-particle deposition of ceramics using electrostatic atomization. *J. Mater. Sci. Lett.* **1997**, *16*, 1017–1019. [CrossRef]

38. Tinkov, S.; Bekeredjian, R.; Winter, G.; Coester, C. Microbubbles as ultrasound triggered drug carriers. *J. Pharm. Sci.* **2009**, *98*, 1935–1961. [CrossRef]

39. Surya, V.; Manaz, M.; Sharon, P.; Shanmugam, K. Ultrasound-Targeted Microbubble Destruction (UTMD): Targeted Nanodrug Delivery in Cancer. *BOHR Int. J. Cancer Res.* **2022**, *1*, 13–15.

40. He, J.; Liu, Z.; Zhu, X.; Xia, H.; Gao, H.; Lu, J. Ultrasonic Microbubble Cavitation Enhanced Tissue Permeability and Drug Diffusion in Solid Tumor Therapy. *Pharmaceutics* **2022**, *14*, 1642. [CrossRef]

41. Yang, F.Y.; Wang, H.E.; Lin, G.L.; Teng, M.C.; Lin, H.H.; Wong, T.T.; Liu, R.S. Micro-SPECT/CT-based pharmacokinetic analysis of 99mTc-diethylenetriaminepentaacetic acid in rats with blood-brain barrier disruption induced by focused ultrasound. *J. Nucl. Med.* **2011**, *52*, 478–484. [CrossRef] [PubMed]

42. Tung, Y.S.; Vlachos, F.; Feshitan, J.A.; Borden, M.A.; Konofagou, E.E. The mechanism of interaction between focused ultrasound and microbubbles in blood-brain barrier opening in mice. *J. Acoust. Soc. Am.* **2011**, *130*, 3059–3067. [CrossRef] [PubMed]

43. Singh, B.; Shukla, N.; Cho, C.-H.; Kim, B.S.; Park, M.-H.; Kim, K. Effect and application of micro- and nanobubbles in water purification. *Toxicol. Environ. Health Sci.* **2021**, *13*, 9–16. [CrossRef]

44. Kamaev, P.P.; Hutcheson, J.D.; Wilson, M.L.; Prausnitz, M.R. Quantification of Optison bubble size and lifetime during sonication dominant role of secondary cavitation bubbles causing acoustic bioeffects. *J. Acoust. Soc. Am.* **2004**, *115*, 1818–1825. [CrossRef] [PubMed]

45. Azmin, M.; Harfield, C.; Ahmad, Z.; Edirisinghe, M.; Stride, E. How do microbubbles and ultrasound interact? Basic physical, dynamic and engineering principles. *Curr. Pharm. Design* **2012**, *18*, 2118–2134. [CrossRef]

46. Jangjou, A.; Meisami, A.H.; Jamali, K.; Niakan, M.H.; Abbasi, M.; Shafiee, M.; Salehi, M.; Hosseinzadeh, A.; Amani, A.M.; Vaez, A. The promising shadow of microbubble over medical sciences: From fighting wide scope of prevalence disease to cancer eradication. *J. Biomed. Sci.* **2021**, *28*, 49. [CrossRef] [PubMed]

47. Abrahao, A.; Meng, Y.; Llinas, M.; Huang, Y.; Hamani, C.; Mainprize, T.; Aubert, I.; Heyn, C.; Black, S.E.; Hynynen, K.; et al. First-in-human trial of blood-brain barrier opening in amyotrophic lateral sclerosis using MR-guided focused ultrasound. *Nat. Commun.* **2019**, *10*, 4373. [CrossRef]

48. Zhan, W. Effects of Focused-Ultrasound-and-Microbubble-Induced Blood-Brain Barrier Disruption on Drug Transport under Liposome-Mediated Delivery in Brain Tumour: A Pilot Numerical Simulation Study. *Pharmaceutics* **2020**, *12*, 69. [CrossRef]

49. Lipsman, N.; Meng, Y.; Bethune, A.J.; Huang, Y.; Lam, B.; Masellis, M.; Herrmann, N.; Heyn, C.; Aubert, I.; Boutet, A.; et al. Blood-brain barrier opening in Alzheimer's disease using MR-guided focused ultrasound. *Nat. Commun.* **2018**, *9*, 2336. [CrossRef]

50. Stride, E.; Edirisinghe, M. Novel preparation techniques for controlling microbubble uniformity: A comparison. *Med. Biol. Eng. Comput.* **2009**, *47*, 883–892. [CrossRef]

51. Roovers, S.; Segers, T.; Lajoinie, G.; Deprez, J.; Versluis, M.; De Smedt, S.C.; Lentacker, I. The Role of Ultrasound-Driven Microbubble Dynamics in Drug Delivery: From Microbubble Fundamentals to Clinical Translation. *Langmuir* **2019**, *35*, 10173–10191. [CrossRef] [PubMed]

52. Sheeran, P.S.; Matsunaga, T.O.; Dayton, P.A. Phase change events of volatile liquid perfluorocarbon contrast agents produce unique acoustic signatures. *Phys. Med. Biol.* **2014**, *59*, 379–401. [CrossRef] [PubMed]

53. Su, C.; Ren, X.; Nie, F.; Li, T.; Lv, W.; Li, H.; Zhang, Y. Current advances in ultrasound-combined nanobubbles for cancer-targeted therapy: A review of the current status and future perspectives. *RSC Adv.* **2021**, *11*, 12915–12928. [CrossRef] [PubMed]

54. Stride, E.; Segers, T.; Lajoinie, G.; Cherkaoui, S.; Bettinger, T.; Versluis, M.; Borden, M. Microbubble agents: New directions. *Ultrasound Med. Biol.* **2020**, *46*, 1326–1343. [CrossRef]

55. Abou-Saleh, R.H.; McLaughlan, J.R.; Bushby, R.J.; Johnson, B.R.; Freear, S.; Evans, S.D.; Thomson, N.H. Molecular Effects of Glycerol on Lipid Monolayers at the Gas-Liquid Interface: Impact on Microbubble Physical and Mechanical Properties. *Langmuir* **2019**, *35*, 10097–10105. [CrossRef]

56. Tran, W.T.; Iradji, S.; Sofroni, E.; Giles, A.; Eddy, D.; Czarnota, G.J. Microbubble and ultrasound radioenhancement of bladder cancer. *Br. J. Cancer* **2012**, *107*, 469–476. [CrossRef]

57. Wu, T.; Huang, C.; Yao, Y.; Du, Z.; Liu, Z. Suicide Gene Delivery System Mediated by Ultrasound-Targeted Microbubble Destruction: A Promising Strategy for Cancer Therapy. *Hum. Gene. Ther.* **2022**, *33*, 1246–1259. [CrossRef]

58. Fan, C.H.; Wang, T.W.; Hsieh, Y.K.; Wang, C.F.; Gao, Z.; Kim, A.; Nagasaki, Y.; Yeh, C.K. Enhancing Boron Uptake in Brain Glioma by a Boron-Polymer/Microbubble Complex with Focused Ultrasound. *ACS Appl. Mater. Interfaces* **2019**, *11*, 11144–11156. [CrossRef]

59. Schwendener, R.A.; Schott, H. Liposome Formulations of Hydrophobic Drugs. *Methods Mol. Biol.* **2017**, *1522*, 73–82.

60. Prasad, C.; Banerjee, R. Ultrasound-Triggered Spatiotemporal Delivery of Topotecan and Curcumin as Combination Therapy for Cancer. *J. Pharmacol. Exp. Ther.* **2019**, *370*, 876–893. [CrossRef]

61. Al-Jawadi, S.; Thakur, S.S. Ultrasound-responsive lipid microbubbles for drug delivery: A review of preparation techniques to optimise formulation size, stability and drug loading. *Int. J. Pharm.* **2020**, *585*, 119559. [CrossRef] [PubMed]

62. Chang, E.L.; Ting, C.Y.; Hsu, P.H.; Lin, Y.C.; Liao, E.C.; Huang, C.Y.; Chang, Y.C.; Chan, H.L.; Chiang, C.S.; Liu, H.L.; et al. Angiogenesis-targeting microbubbles combined with ultrasound-mediated gene therapy in brain tumors. *J. Control. Release* **2017**, *255*, 164–175. [CrossRef] [PubMed]

63. Fan, C.H.; Cheng, Y.H.; Ting, C.Y.; Ho, Y.J.; Hsu, P.H.; Liu, H.L.; Yeh, C.K. Ultrasound/Magnetic Targeting with SPIO-DOX-Microbubble Complex for Image-Guided Drug Delivery in Brain Tumors. *Theranostics* **2016**, *6*, 1542–1556. [CrossRef] [PubMed]

64. Ting, C.Y.; Fan, C.H.; Liu, H.L.; Huang, C.Y.; Hsieh, H.Y.; Yen, T.C.; Wei, K.C.; Yeh, C.K. Concurrent blood-brain barrier opening and local drug delivery using drug-carrying microbubbles and focused ultrasound for brain glioma treatment. *Biomaterials* **2012**, *33*, 704–712. [CrossRef]

65. Fan, C.H.; Ting, C.Y.; Liu, H.L.; Huang, C.Y.; Hsieh, H.Y.; Yen, T.C.; Wei, K.C.; Yeh, C.K. Antiangiogenic-targeting drug-loaded microbubbles combined with focused ultrasound for glioma treatment. *Biomaterials* **2013**, *34*, 2142–2155. [CrossRef]

66. Ha, S.W.; Hwang, K.; Jin, J.; Cho, A.S.; Kim, T.Y.; Hwang, S.I.; Lee, H.J.; Kim, C.Y. Ultrasound-sensitizing nanoparticle complex for overcoming the blood-brain barrier: An effective drug delivery system. *Int. J. Nanomed.* **2019**, *14*, 3743–3752. [CrossRef]

67. Zhao, G.; Huang, Q.; Wang, F.; Zhang, X.; Hu, J.; Tan, Y.; Huang, N.; Wang, Z.; Wang, Z.; Cheng, Y. Targeted shRNA-loaded liposome complex combined with focused ultrasound for blood brain barrier disruption and suppressing glioma growth. *Cancer Lett.* **2018**, *418*, 147–158. [CrossRef] [PubMed]

68. Yang, F.Y.; Lin, G.L.; Horng, S.C.; Chang, T.K.; Wu, S.Y.; Wong, T.T.; Wang, H.E. Pulsed high-intensity focused ultrasound enhances the relative permeability of the blood-tumor barrier in a glioma-bearing rat model. *IEEE Trans. Ultrason. Ferroelectr. Freq. Control* **2011**, *58*, 964–970. [CrossRef]

69. Dong, L.; Li, N.; Wei, X.; Wang, Y.; Chang, L.; Wu, H.; Song, L.; Guo, K.; Chang, Y.; Yin, Y.; et al. A Gambogic Acid-Loaded Delivery System Mediated by Ultrasound-Targeted Microbubble Destruction: A Promising Therapy Method for Malignant Cerebral Glioma. *Int. J. Nanomed.* **2022**, *17*, 2001–2017. [CrossRef]

70. Park, S.H.; Yoon, Y.I.; Moon, H.; Lee, G.H.; Lee, B.H.; Yoon, T.J.; Lee, H.J. Development of a novel microbubble-liposome complex conjugated with peptide ligands targeting IL4R on brain tumor cells. *Oncol. Rep.* **2016**, *36*, 131–136. [CrossRef]

71. Zhao, Y.-Z.; Liang, H.-D.; Mei, X.-G.; Halliwell, M. Preparation, characterization and in vivo observation of phospholipid-based gas-filled microbubbles containing hirudin. *Ultrasound Med. Biol.* **2005**, *31*, 1237–1243. [CrossRef] [PubMed]

72. Christiansen, C.; Kryvi, H.; Sontum, P.; Skotland, T. Physical and biochemical characterization of Albunex, a new ultrasound contrast agent consisting of air-filled albumin microspheres suspended in a solution of human albumin. *Biotechnol. Appl. Biochem.* **1994**, *19*, 307–320. [PubMed]

73. Unger, E.C.; McCreery, T.P.; Sweitzer, R.H.; Caldwell, V.E.; Wu, Y. Acoustically active liposheres containing paclitaxel: A new therapeutic ultrasound contrast agent. *Investig. Radiol.* **1998**, *33*, 886–892. [CrossRef] [PubMed]

74. Yoon, Y.I.; Kwon, Y.S.; Cho, H.S.; Heo, S.H.; Park, K.S.; Park, S.G.; Lee, S.H.; Hwang, S.I.; Kim, Y.I.; Jae, H.J.; et al. Ultrasound-mediated gene and drug delivery using a microbubble-liposome particle system. *Theranostics* **2014**, *4*, 1133–1144. [CrossRef] [PubMed]

75. Li, H.; Yang, Y.; Zhang, M.; Yin, L.; Tu, J.; Guo, X.; Zhang, D. Acoustic Characterization and Enhanced Ultrasound Imaging of Long-Circulating Lipid-Coated Microbubbles. *J. Ultrasound Med.* **2018**, *37*, 1243–1256. [CrossRef]

76. Xie, B.; Zhou, C.; Chen, J.; Huang, X.; Zhang, J. Preparation of microbubbles with the generation of Dean vortices in a porous membrane. *Chem. Eng. Sci.* **2022**, *247*, 117105. [CrossRef]

77. Melich, R.; Valour, J.-P.; Urbaniak, S.; Padilla, F.; Charcosset, C. Preparation and characterization of perfluorocarbon microbubbles using Shirasu Porous Glass (SPG) membranes. *Colloids Surf. A Physicochem. Eng. Asp.* **2019**, *560*, 233–243. [CrossRef]

78. Segers, T.; de Rond, L.; de Jong, N.; Borden, M.; Versluis, M. Stability of Monodisperse Phospholipid-Coated Microbubbles Formed by Flow-Focusing at High Production Rates. *Langmuir* **2016**, *32*, 3937–3944. [CrossRef]

79. Dhanaliwala, A.H.; Dixon, A.J.; Lin, D.; Chen, J.L.; Klibanov, A.L.; Hossack, J.A. In vivo imaging of microfluidic-produced microbubbles. *Biomed. Microdevices* **2015**, *17*, 23. [CrossRef]

80. Pulsipher, K.W.; Hammer, D.A.; Lee, D.; Sehgal, C.M. Engineering Theranostic Microbubbles Using Microfluidics for Ultrasound Imaging and Therapy: A Review. *Ultrasound Med. Biol.* **2018**, *44*, 2441–2460. [CrossRef]

81. Churchman, A.H.; Mico, V.; de Pablo, J.G.; Peyman, S.A.; Freear, S.; Evans, S.D. Combined flow-focus and self-assembly routes for the formation of lipid stabilized oil-shelled microbubbles. *Microsyst. Nanoeng.* **2018**, *4*, 1–8. [CrossRef]

82. Tsai, H.C.; Tsai, C.H.; Chen, W.S.; Inserra, C.; Wei, K.C.; Liu, H.L. Safety evaluation of frequent application of microbubble-enhanced focused ultrasound blood-brain-barrier opening. *Sci. Rep.* **2018**, *8*, 17720. [CrossRef]

83. Choi, J.J.; Feshitan, J.A.; Baseri, B.; Wang, S.; Tung, Y.S.; Borden, M.A.; Konofagou, E.E. Microbubble-size dependence of focused ultrasound-induced blood-brain barrier opening in mice in vivo. *IEEE Trans. Biomed. Eng.* **2010**, *57*, 145–154. [CrossRef] [PubMed]

84. Liu, H.L.; Hua, M.Y.; Yang, H.W.; Huang, C.Y.; Chu, P.C.; Wu, J.S.; Tseng, I.C.; Wang, J.J.; Yen, T.C.; Chen, P.Y.; et al. Magnetic resonance monitoring of focused ultrasound/magnetic nanoparticle targeting delivery of therapeutic agents to the brain. *Proc. Natl. Acad. Sci. USA* **2010**, *107*, 15205–15210. [CrossRef] [PubMed]

85. Treat, L.H.; Zhang, Y.; McDannold, N.; Hynynen, K. Impact of Focused Ultrasound-Enhanced Drug Delivery on Survival in Rats with Glioma. In *AIP Conference Proceedings*; American Institute of Physics: College Park, MD, USA, 2009; pp. 443–447.

86. Lentacker, I.; De Smedt, S.C.; Sanders, N.N. Drug loaded microbubble design for ultrasound triggered delivery. *Soft Matter.* **2009**, *5*, 2161–2170. [CrossRef]

87. Singh, B.; Lee, J.; Kim, H.-G.; Park, M.-H.; Kim, K. Colorimetric detection of copper ions using porphyrin-conjugated silica nanoparticles. *Toxicol. Environ. Health Sci.* **2020**, *12*, 381–389. [CrossRef]

88. Thomas, A.P.; Lee, A.J.; Palanikumar, L.; Jana, B.; Kim, K.; Kim, S.; Ok, H.; Seol, J.; Kim, D.; Kang, B.H.; et al. Mitochondrial heat shock protein-guided photodynamic therapy. *Chem. Commun.* **2019**, *55*, 12631–12634. [CrossRef] [PubMed]

89. Tsutsui, J.M.; Xie, F.; Porter, R.T. The use of microbubbles to target drug delivery. *Cardiovasc. Ultrasound* **2004**, *2*, 1–7. [CrossRef]

90. Tu, J.; Zhang, H.; Yu, J.; Liufu, C.; Chen, Z. Ultrasound-mediated microbubble destruction: A new method in cancer immunotherapy. *Onco Targets Ther.* **2018**, *11*, 5763–5775. [CrossRef]

91. Wei, K.C.; Chu, P.C.; Wang, H.Y.; Huang, C.Y.; Chen, P.Y.; Tsai, H.C.; Lu, Y.J.; Lee, P.Y.; Tseng, I.C.; Feng, L.Y.; et al. Focused ultrasound-induced blood-brain barrier opening to enhance temozolomide delivery for glioblastoma treatment: A preclinical study. *PLoS ONE* **2013**, *8*, e58995. [CrossRef]

92. Yang, F.Y.; Wong, T.T.; Teng, M.C.; Liu, R.S.; Lu, M.; Liang, H.F.; Wei, M.C. Focused ultrasound and interleukin-4 receptor-targeted liposomal doxorubicin for enhanced targeted drug delivery and antitumor effect in glioblastoma multiforme. *J. Control Release* **2012**, *160*, 652–658. [CrossRef]

93. Wang, F.; Dong, L.; Liang, S.; Wei, X.; Wang, Y.; Chang, L.; Guo, K.; Wu, H.; Chang, Y.; Yin, Y.; et al. Ultrasound-triggered drug delivery for glioma therapy through gambogic acid-loaded nanobubble-microbubble complexes. *Biomed. Pharmacother.* **2022**, *150*, 113042. [CrossRef] [PubMed]

94. Chen, H.; Chen, C.C.; Acosta, C.; Wu, S.Y.; Sun, T.; Konofagou, E.E. A new brain drug delivery strategy: Focused ultrasound-enhanced intranasal drug delivery. *PLoS ONE* **2014**, *9*, e108880. [CrossRef] [PubMed]

95. Chen, P.Y.; Hsieh, H.Y.; Huang, C.Y.; Lin, C.Y.; Wei, K.C.; Liu, H.L. Focused ultrasound-induced blood-brain barrier opening to enhance interleukin-12 delivery for brain tumor immunotherapy: A preclinical feasibility study. *J. Transl. Med.* **2015**, *13*, 93. [CrossRef] [PubMed]

96. McDannold, N.; Zhang, Y.; Supko, J.G.; Power, C.; Sun, T.; Peng, C.; Vykhodtseva, N.; Golby, A.J.; Reardon, D.A. Acoustic feedback enables safe and reliable carboplatin delivery across the blood-brain barrier with a clinical focused ultrasound system and improves survival in a rat glioma model. *Theranostics* **2019**, *9*, 6284–6299. [CrossRef] [PubMed]

97. Yang, F.Y.; Wang, H.E.; Liu, R.S.; Teng, M.C.; Li, J.J.; Lu, M.; Wei, M.C.; Wong, T.T. Pharmacokinetic analysis of 111 in-labeled liposomal Doxorubicin in murine glioblastoma after blood-brain barrier disruption by focused ultrasound. *PLoS ONE* **2012**, *7*, e45468.

98.   Liu, H.L.; Huang, C.Y.; Chen, J.Y.; Wang, H.Y.; Chen, P.Y.; Wei, K.C. Pharmacodynamic and therapeutic investigation of focused ultrasound-induced blood-brain barrier opening for enhanced temozolomide delivery in glioma treatment. *PLoS ONE* **2014**, *9*, e114311. [CrossRef]

99.   Aryal, M.; Vykhodtseva, N.; Zhang, Y.Z.; Park, J.; McDannold, N. Multiple treatments with liposomal doxorubicin and ultrasound-induced disruption of blood-tumor and blood-brain barriers improve outcomes in a rat glioma model. *J. Control. Release* **2013**, *169*, 103–111. [CrossRef]

100. Zhang, J.; Liu, H.; Du, X.; Guo, Y.; Chen, X.; Wang, S.; Fang, J.; Cao, P.; Zhang, B.; Liu, Z.; et al. Increasing of Blood-Brain Tumor Barrier Permeability through Transcellular and Paracellular Pathways by Microbubble-Enhanced Diagnostic Ultrasound in a C6 Glioma Model. *Front. Neurosci.* **2017**, *11*, 86. [CrossRef]

101. Treat, L.H.; McDannold, N.; Zhang, Y.; Vykhodtseva, N.; Hynynen, K. Improved anti-tumor effect of liposomal doxorubicin after targeted blood-brain barrier disruption by MRI-guided focused ultrasound in rat glioma. *Ultrasound Med. Biol.* **2012**, *38*, 1716–1725. [CrossRef]

102. Zhang, D.Y.; Dmello, C.; Chen, L.; Arrieta, V.A.; Gonzalez-Buendia, E.; Kane, J.R.; Magnusson, L.P.; Baran, A.; James, C.D.; Horbinski, C.; et al. Ultrasound-mediated Delivery of Paclitaxel for Glioma: A Comparative Study of Distribution, Toxicity, and Efficacy of Albumin-bound Versus Cremophor Formulations. *Clin. Cancer Res.* **2020**, *26*, 477–486. [CrossRef] [PubMed]

103. Sun, T.; Zhang, Y.; Power, C.; Alexander, P.M.; Sutton, J.T.; Aryal, M.; Vykhodtseva, N.; Miller, E.L.; McDannold, N.J. Closed-loop control of targeted ultrasound drug delivery across the blood-brain/tumor barriers in a rat glioma model. *Proc. Natl. Acad. Sci. USA* **2017**, *114*, E10281–E10290. [CrossRef]

104. Moon, H.; Hwang, K.; Nam, K.M.; Kim, Y.S.; Ko, M.J.; Kim, H.R.; Lee, H.J.; Kim, M.J.; Kim, T.H.; Kang, K.S.; et al. Enhanced delivery to brain using sonosensitive liposome and microbubble with focused ultrasound. *Biomater. Adv.* **2022**, *141*, 213102. [CrossRef]

105. Dong, Y.; Wong, J.S.L.; Sugimura, R.; Lam, K.O.; Li, B.; Kwok, G.G.W.; Leung, R.; Chiu, J.W.Y.; Cheung, T.T.; Yau, T. Recent Advances and Future Prospects in Immune Checkpoint (ICI)-Based Combination Therapy for Advanced HCC. *Cancers* **2021**, *13*, 1949. [CrossRef] [PubMed]

106. Brueckl, W.M.; Ficker, J.H.; Zeitler, G. Clinically relevant prognostic and predictive markers for immune-checkpoint-inhibitor (ICI) therapy in non-small cell lung cancer (NSCLC). *BMC Cancer* **2020**, *20*, 1185. [CrossRef] [PubMed]

107. Gong, Y.; Ye, D.; Chien, C.Y.; Yue, Y.; Chen, H. Comparison of Sonication Patterns and Microbubble Administration Strategies for Focused Ultrasound-Mediated Large-Volume Drug Delivery. *IEEE Trans. Biomed. Eng.* **2022**, *69*, 3449–3459. [CrossRef] [PubMed]

108. Alkins, R.; Burgess, A.; Kerbel, R.; Wels, W.S.; Hynynen, K. Early treatment of HER2-amplified brain tumors with targeted NK-92 cells and focused ultrasound improves survival. *Neuro. Oncol.* **2016**, *18*, 974–981. [CrossRef] [PubMed]

109. Zhang, X.; Ye, D.; Yang, L.; Yue, Y.; Sultan, D.; Pacia, C.P.; Pang, H.; Detering, L.; Heo, G.S.; Luehmann, H.; et al. Magnetic Resonance Imaging-Guided Focused Ultrasound-Based Delivery of Radiolabeled Copper Nanoclusters to Diffuse Intrinsic Pontine Glioma. *ACS Appl. Nano Mater.* **2020**, *3*, 11129–11134. [CrossRef]

110. Ye, D.; Sultan, D.; Zhang, X.; Yue, Y.; Heo, G.S.; Kothapalli, S.; Luehmann, H.; Tai, Y.C.; Rubin, J.B.; Liu, Y.; et al. Focused ultrasound-enabled delivery of radiolabeled nanoclusters to the pons. *J. Control. Release* **2018**, *283*, 143–150. [CrossRef]

111. Chen, P.Y.; Liu, H.L.; Hua, M.Y.; Yang, H.W.; Huang, C.Y.; Chu, P.C.; Lyu, L.A.; Tseng, I.C.; Feng, L.Y.; Tsai, H.C.; et al. Novel magnetic/ultrasound focusing system enhances nanoparticle drug delivery for glioma treatment. *Neuro. Oncol.* **2010**, *12*, 1050–1060. [CrossRef]

112. Wu, S.Y.; Chen, C.C.; Tung, Y.S.; Olumolade, O.O.; Konofagou, E.E. Effects of the microbubble shell physicochemical properties on ultrasound-mediated drug delivery to the brain. *J. Control. Release* **2015**, *212*, 30–40. [CrossRef] [PubMed]

113. Dymova, M.A.; Taskaev, S.Y.; Richter, V.A.; Kuligina, E.V. Boron neutron capture therapy: Current status and future perspectives. *Cancer Commun.* **2020**, *40*, 406–421. [CrossRef] [PubMed]

114. Nedunchezhian, K.; Aswath, N.; Thiruppathy, M.; Thirugnanamurthy, S. Boron Neutron Capture Therapy–A Literature Review. *J. Clin. Diagn Res.* **2016**, *10*, ZE01–ZE04. [CrossRef] [PubMed]

115. Fan, C.H.; Ting, C.Y.; Lin, H.J.; Wang, C.H.; Liu, H.L.; Yen, T.C.; Yeh, C.K. SPIO-conjugated, doxorubicin-loaded microbubbles for concurrent MRI and focused-ultrasound enhanced brain-tumor drug delivery. *Biomaterials* **2013**, *34*, 3706–3715. [CrossRef] [PubMed]

116. Liu, H.-L.; Hua, M.-Y.; Chen, P.-Y.; Chu, P.-C.; Pan, C.-H.; Yang, H.-W.; Huang, C.-Y.; Wang, J.-J.; Yen, T.-C.; Wei, K.-C.J.R. Blood-brain barrier disruption with focused ultrasound enhances delivery of chemotherapeutic drugs for glioblastoma treatment. *Radiology* **2010**, *255*, 415–425. [CrossRef]